

https://doi.org/10.1070/QEL16991

The role of dispersion in the mechanism of femtosecond pulse self-shortening in Kerr media

Ya.V. Grudtsyn, A.V. Koribut, L.D. Mikheev, V.A. Trofimov, V.I. Yalovoi

Abstract. **We investigate the influence of material dispersion on the mechanism of self-shortening of femtosecond pulses interacting with fused silica plates having thicknesses an order of magnitude smaller than the dispersion length for the initial 72-fs pulse. The femtosecond pulse self-shortening is observed at large values of the *B* integral, when small-scale self-focusing develops in the central part of the pulse; this self-focusing plays the role of an optical shutter selecting the unperturbed radiation of the pulse leading edge. A study of the femtosecond pulse self-shortening in 1- and 3-mm-thick fused silica samples reveals that, under the experimental conditions in use, the self-phase modulation enhances the role of dispersion in the formation of a shortened pulse. With an increase in the sample thickness, the shortened pulse width increases as a result of the dispersion spread of the initial pulse in time. At the same time, this shortened pulse remains close to the transform-limited one, independent of the sample thickness.**

Keywords: *self-shortening, femtosecond pulses, small-scale self-focusing, modulational instability, nonlinear Schrödinger equation.*

1. Introduction

Currently, various applications in fundamental and applied physics [1–3] call for few-cycle pulses. However, because of the regenerative narrowing of the spectrum during amplification, it is difficult to obtain pulses shorter than 20–30 fs directly at the output of multiterawatt and petawatt solid-state systems. To form such few-cycle high-energy pulses, it is necessary to develop extracavity compression techniques [4, 5]. Most of the methods of pulse shortening are based on the use of self-phase modulation (SPM) for pulse spectral broadening with subsequent compensation for the acquired nonlinear phase by dispersion elements. In some cases, a pulse close to a transform-limited one is formed directly as a result of nonlinear interaction (self-compression). The self-compression methods known to date are characterised by limited energy scalability [6, 7].

Previously we described the effect of femtosecond pulse self-shortening in fused silica glass at the second-harmonic wavelength of a Ti:sapphire system ($\lambda = 475$ nm) [8–12]. This effect is due to the development of small-scale self-focusing in the central part of the pulse and the formation of plasma channels (caused by this self-focusing), which remain until the end of the pulse. As a result, the central part and trailing edge of the pulse undergo strong angular loss due to the refraction from refractive index inhomogeneities, which are caused by the Kerr nonlinearity and plasma, while the unperturbed leading edge of the pulse forms a shorter (close to transform-limited) pulse in the far-field zone [11, 12]. The physical nature of this pulse self-shortening mechanism is such that it has no limitations on the beam energy scalability (with conservation of necessary intensity on the sample surface), and there are prospects for its further development for generating few-cycle pulses. One of the conditions for making this method maximally efficient is the absence of influence of material dispersion on the self-shortening mechanism; the role of material dispersion is the object of our study.

2. Experimental results and discussion

A schematic of the experimental setup is presented in Fig. 1. The parameters of the radiation interacting with samples are as follows: the pulse energy is up to 200 μJ, the FWHM of transform-limited pulse is $T_{1/2} = 72$ fs, and the centre wavelength is 471 nm (Fig. 2). The samples under study were KU-1 fused silica plates with thicknesses of 1 and 3 mm. The intensity of the radiation interacting with samples was varied within 1–2.9 TW cm^{-2} by shifting the sample along the convergent beam axis. The radiation of the central part of the beam, with an approximately homogeneous spatial intensity distribution, was cut by diaphragms 60 and 100 μm in diam-

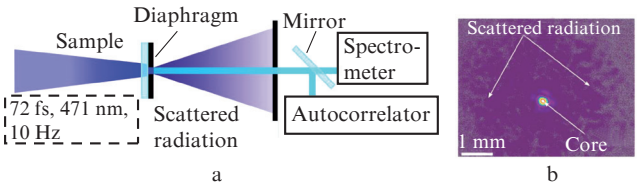

Figure 1. (a) Schematic of the setup for studying the interaction of a transform-limited pulse with a thin fused silica sample and (b) the beam profile behind the diaphragm (intensity 2.9 TW cm^{-2}, 1-mm-thick fused silica sample).

Ya.V. Grudtsyn, A.V. Koribut, V.I. Yalovoi P.N. Lebedev Physical Institute, Russian Academy of Sciences, Leninsky prosp. 53, 119991 Moscow, Russia; e-mail: jgrudtsin@gmail.com, andrew-koribut@yandex.ru, yalovoy@sci.lebedev.ru;
L.D. Mikheev P.N. Lebedev Physical Institute, Russian Academy of Sciences, Leninsky prosp. 53, 119991 Moscow, Russia; National Research Nuclear University 'MEPhI' (Moscow Engineering Physics Institute), Kashirskoe sh. 31, 115409 Moscow, Russia; e-mail: mikheev@sci.lebedev.ru;
V.A. Trofimov Faculty of Computational Mathematics and Cybernetics, M.V. Lomonosov Moscow State University, Vorob'evy gory, 119991 Moscow, Russia; e-mail: vatro@cs.msu.ru

Received 6 March 2019
Kvantovaya Elektronika **49** (4) 302–306 (2019)
Translated by Yu.P. Sin'kov

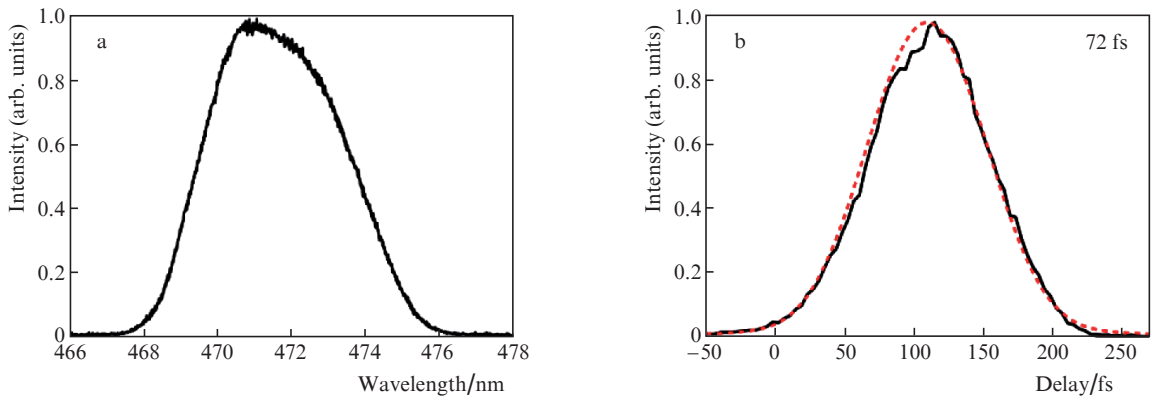

Figure 2. (a) Spectrum and (b) autocorrelation function of the initial pulse: (dotted line) result of calculation (reverse Fourier transform of the pulse spectrum) and (solid lines) experimental data.

eter, installed directly after the 1- and 3-mm-thick plates, respectively. The beam behind the diaphragm consisted of a core, whose size was independent of the initial radiation intensity, and scattered radiation with a divergence angle of up to 0.1 rad (the convergence angle of the initial beam was 0.01 rad).

When the radiation with an intensity of 2.9 TW cm^{-2} interacted with the 1-mm-thick sample, the pulse width was reduced to 20 fs, the spectrum was broadened, and its maximum was red-shifted to 490 nm (Fig. 3a). A similar phenomenon was observed when radiation with an intensity of 1.1 TW cm^{-2} interacted with the 3-mm-thick sample (Fig. 3b); however, the pulse width decreased in this case to only 32 fs, and the spectral shift was smaller. The autocorrelation functions presented in Fig. 3, which were obtained using a reverse Fourier transform from the pulse spectra, almost coincide with the experimental curves, thus indicating that the shortened pulses are close to transform-limited ones.

The development of small-scale self-focusing, which leads to pulse shortening, is due to the transverse beam instability [13]. The noise gain throughout the entire sample thickness is determined by the B integral, which can be estimated as $(2\pi/\lambda) \times n_2 IL$,, where n_2 is the nonlinear refractive index, I is intensity, and L is the sample thickness. Under our experimental conditions, the B integral was estimated to be 7.3 and 7.7 for samples with thicknesses of 1 and 3 mm, respectively. It is

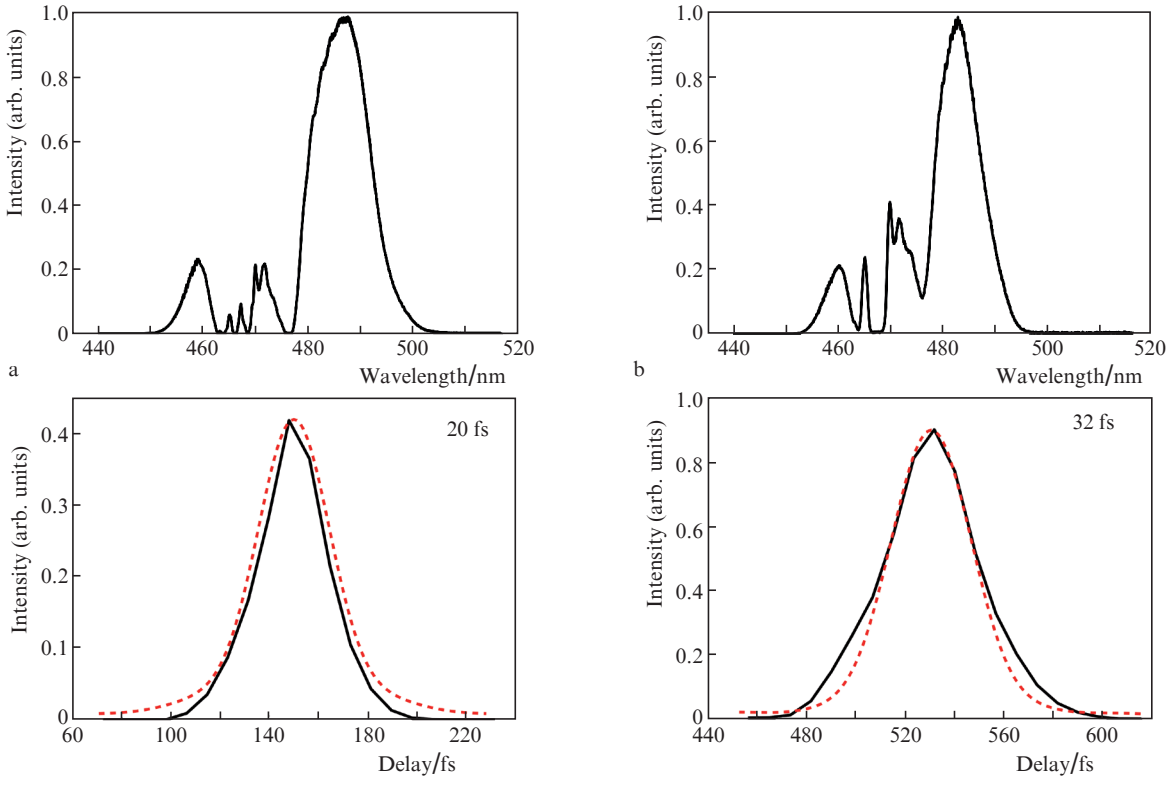

Figure 3. Spectra and autocorrelation functions of radiation in the core (far-field zone after the diaphragm) for fused silica samples with thicknesses of (a) 1 mm (intensity 2.9 TW cm^{-2}) and (b) 3 mm (intensity 1.1 TW cm^{-2}). Dotted lines are calculation results (obtained by inverse Fourier transform of pulse spectra) and solid lines are experimental data.

noteworthy that the thickness of the samples used was much smaller than the dispersion length $L_{dis} = T_{1/2}^2/(4\ln 2\,|k^{(2)}|)$ [$k^{(2)}$ is the group-velocity dispersion parameter] for a 72-fs pulse: 2.5 cm in fused silica. At first glance, it appears unlikely that a change in thickness in the range under consideration may affect significantly self-shortening. However, the effect of SPM increases the role of dispersion in self-shortening and, as will be shown below, reduces the B integral because of the temporal broadening of the initial pulse.

The experimental results were analysed with allowance for dispersion based on the numerical simulation of nonlinear propagation of femtosecond radiation in a Kerr medium using the axially symmetric model of radiation interaction with optically transparent media, which was developed jointly with the Laboratory of Mathematical Modelling in Physics (Moscow State University). The model is based on solving the nonlinear Schrödinger equation derived in the slowly-varying wave approximation [14] and supplemented with the plasma formation process [15]:

$$\frac{\partial}{\partial\xi}A = \frac{i\Delta_\perp}{2k_0}A - \frac{ik^{(2)}}{2}\frac{\partial^2}{\partial\tau^2}A + \frac{ik_0^2 n_2}{n_0}\left(1 + \frac{i}{\omega_0}\frac{\partial}{\partial\tau}\right)$$

$$\times\left[\int_0^\infty R(t')\,|A(\tau - t')|^2\,dt'\right]A - \frac{ik_0}{2n_0^2\rho_c}\left(1 - \frac{i}{\omega_0}\frac{\partial}{\partial\tau}\right)\rho_e A -$$

$$-\frac{1}{2}(\sigma\rho_e A + \beta_K\,|A|^{2(K-1)}A),$$

$$\frac{\partial}{\partial\tau}\rho_e = \frac{\sigma_K}{(\hbar\omega_0)^K}\rho_{nt}\,|A|^{2K} + \frac{\sigma}{U_i}\rho_e\,|A|^2 - \frac{1}{\tau_r}\rho_e.$$

Here, $A(\tau, r, \xi)$ is the complex electric field envelope; ω_0 is the centre frequency of the initial pulse spectrum; k_0 is the wavenumber; $\tau = t - z/u$ and $\xi = z$ are, respectively, the time and longitudinal coordinate in a moving coordinate system (u is the group velocity, t and z are the time and longitudinal coordinate in the system at rest); $K = 4$ is the order of multiphoton absorption; $\rho_e(\tau, r, \xi)$ is the free-charge concentration; σ_K is the four-photon absorption cross section; U_i is the band gap; τ_r is the free-charge recombination time; ρ_{nt} is the concentration of material; σ is the inverse bremsstrahlung absorption cross section; n_0 is the refractive index; β_K is the four-photon absorption coefficient; ρ_c is the critical plasma density; and $R(t)$ is the molecular response function.

This model takes into account the diffraction, dispersion, Kerr nonlinearity, self-steepening, stimulated Raman scattering, and multiphoton and inverse bremsstrahlung absorption, as well as the influence of plasma on the refractive index. However, in view of the axial symmetry, the model does not allow one to perform a complete numerical calculation describing the development of multiple filamentation in the entire beam; therefore, we modelled for simplicity the development of a single perturbation on the beam axis with a transverse size much smaller than the beam diameter. This model and the parameters entering it were described in more detail in [12].

Figure 4 shows as an example the results of calculating the spatiotemporal intensity distributions at the output of the 1-mm-thick sample, which demonstrates beam focusing in the central part of the pulse. The trailing-edge radiation undergoes refraction in the newly formed plasma, while the leading-edge radiation remains unperturbed. The numerically calculated and measured spectra of shortened pulses are compared in Fig. 5; one can see good agreement between the calculation results and experimental data.

Figure 6 shows the calculated temporal intensity profiles and nonlinear phase derivative $d\phi_{n1}/dt$ ($\phi_{n1} = f(\omega_0/c)n_2 I(t)dz$) at the output of 1- and 3-mm-thick samples in the paraxial region of the beam. The maximum value of $d\phi_{n1}/dt$ at the

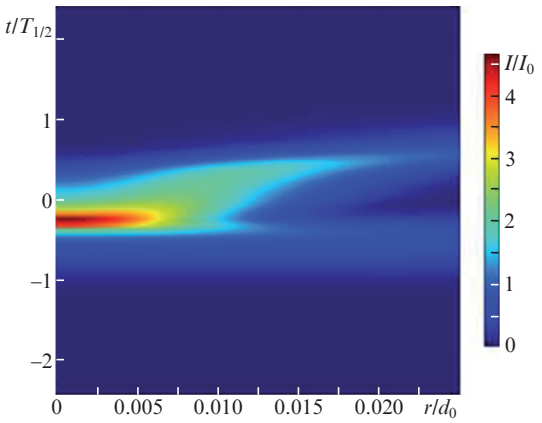

Figure 4. Calculated spatial and temporal intensity distribution at the output of 1-mm-thick sample, demonstrating the occurrence of self-focusing (d_0 is the initial beam diameter at the level of 1/2).

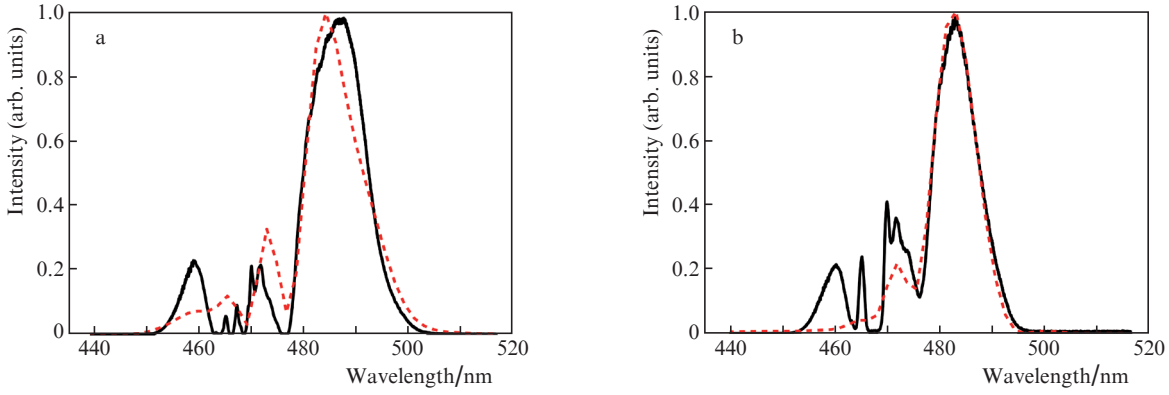

Figure 5. Comparison of the experimental (solid lines) and numerically calculated (dotted lines) core spectra after a diaphragm for fused silica samples with thicknesses of (a) 1 mm (intensity 2.9 TW cm^{-2}) and (b) 3 mm (intensity 1.1 TW cm^{-2}).

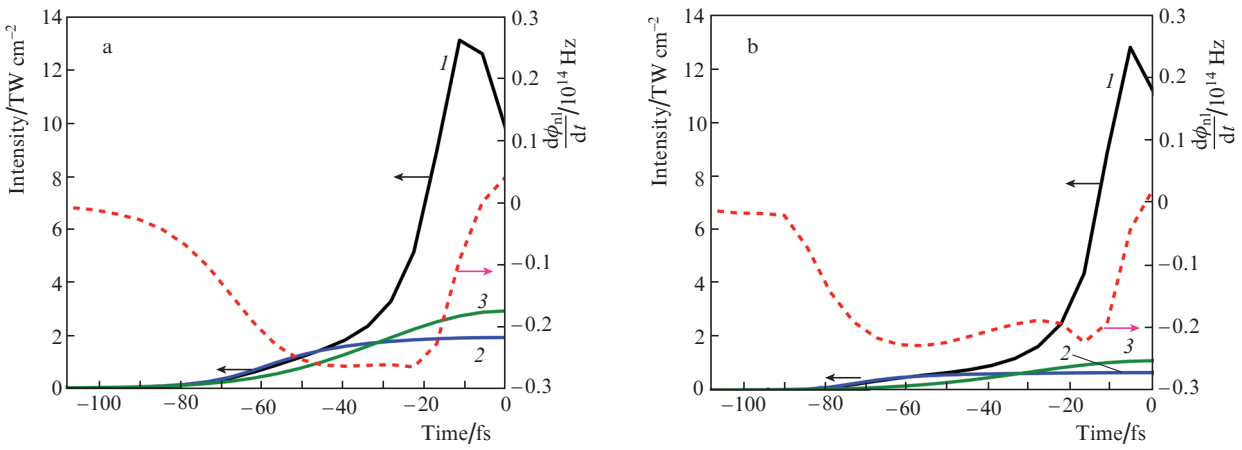

Figure 6. Temporal profiles of the (solid lines) intensity and (dotted lines) nonlinear phase derivative at the output of samples with thicknesses of (a) 1 and (b) 3 mm. (*1*, *2*) Profiles of perturbed and unperturbed intensities, respectively, with dispersion taken into account, and (*3*) intensity profile without perturbation and with dispersion disregarded.

pulse leading edge characterises the spectral shift of the shortened pulse, while the presence of a plateau in the curve $d\phi_{nl}/dt$ indicates possibility of forming transform-limited pulses in the far-field zone behind the sample. A comparison of the temporal profiles of output pulses, which were obtained without intensity perturbation in the initial beam profile (Fig. 6), shows that dispersion causes significant pulse broadening in both samples; in addition, it leads to a larger (by a factor of 1.3) increase in the pulse duration (at half maximum) in the 3-mm-thick sample (GDD = 225 fs^2) in comparison with that in the 1-mm-thick sample (GDD = 75 fs^2) [16]. This gives rise to approximately the same decrease in the nonlinear phase derivative with respect to time at the sample output and, correspondingly, to a spectral shift of the shortened pulse formed at its leading edge.

Thus, the numerical simulation results confirm the important role of material dispersion in the mechanism of femtosecond pulse self-shortening in thin (as compared with the dispersion length) fused silica samples: it leads to a decrease in the self-shortening efficiency with an increase in the sample thickness from 1 to 3 mm. Note that the shortened pulses observed in the far-field are close to transform-limited for both samples. Hence, in the case under consideration, dispersion does not affect the formation conditions for a transform-limited pulse but broadens it due to the spread of the initial pulse in time.

3. Conclusions

It was established that, even when using samples with thicknesses much smaller than the dispersion length for the initial pulse, dispersion plays an important role under the SPM conditions and imposes limitations on the choice of the optimal thickness of the sample applied for femtosecond pulse self-shortening. According to the numerical simulation for the chosen experimental conditions, the dispersion spread of the initial pulse leads to a decrease in the nonlinear phase derivative at the sample output, which corresponds to the experimentally observed decrease in the spectral shift and spectral width of the shortened pulse. The numerical simulation results indicate also that, independent of the sample thickness, the conditions for forming a transform-limited shortened pulse are implemented on the initial-pulse leading edge. This is confirmed by the results of experiments where the shortened pulse widths were close to those of transform-limited pulses for both 1- and 3-mm-thick samples but differed by a factor of 1.5.

Based on the results obtained, we can conclude that optical materials with a high nonlinearity of refractive index and minimally possible group-velocity dispersion are most promising for implementing femtosecond pulse self-shortening. An example of such material for the wavelength range near 480 nm is CaF_2 ($n_2 = 4 \times 10^{-16}$ cm^2 W^{-1} [17] and GVD = 53 fs^2 mm^{-1} [18], whereas for fused silica $n_2 = 2.2 \times 10^{-16}$ cm^2 W^{-1} [19] and GVD = 75 fs^2 mm^{-1} [16]). In this context, note that the aforementioned requirement can more easily be implemented in the near-IR region for the Ti:sapphire laser first harmonic, because in this case the nonlinear refractive index generally does not differ much from the values characteristic of the visible spectral range, whereas the dispersion is much lower.

Acknowledgements. This study was supported by the Presidium of the Russian Academy of Sciences (Fundamental Research Programme "Extreme Light Fields and Their Interaction with Matter) and by the Programme for Increasing the Competitiveness of the National Research Nuclear University 'MEPhI'.

References

1. Kobayashi T., Shirakawa A., Fuji T. *IEEE J. Sel. Top. Quantum Electron.*, **7**, 525 (2001).
2. Zhou M.L., Yan X.Q., Mourou G., Wheeler J.A., Bin J.H., Schreiber J., Tajima T. *Phys. Plasmas*, **23**, 043112 (2016).
3. Witte S., Zinkstok R.T., Hogervorst W., Eikema K.S. *Opt. Express*, **13**, 4903 (2005).
4. Rolland C., Corkum P.B. *J. Opt. Soc. Am. B*, **5**, 641 (1988).
5. Nisoli M., De Silvestri S., Svelto O. *Appl. Phys. Lett.*, **68**, 2793 (1996).
6. Stibenz G., Zhavoronkov N., Steinmeyer G. *Opt. Lett.*, **31**, 274 (2006).
7. Ashihara S., Nishina J., Shimura T., Kuroda K. *J. Opt. Soc. Am. B*, **19**, 2505 (2002).
8. Aristov A.I., Grudtsyn Ya.V., Mikheev L.D., Polivin A.V., Stepanov S.G., Trofimov A.V., Yalovoi V.I. *Quantum Electron.*, **42**, 1097 (2012) [*Kvantovaya Elektron.*, **42**, 1097 (2012)].

9. Alekseev S.V., Aristov A.I., Grudtsyn Ya.V., Ivanov N.G., Koval'chuk B.M., Losev V.F., Mamaev S.B., Mesyats G.A., Mikheev L.D., Panchenko Yu.N., Polivin A.V., Stepanov S.G., Ratakhin N.A., Yalovoi V.I., Yastremskii A.G. *Quantum Electron*., **43**, 190 (2013) [*Kvantovaya Elektron*., **43**, 190 (2013)].
10. Grudtsyn Ya.V., Zubarev I.G., Koribut A.V., Kuchik I.E., Mamaev S.B., Mikheev L.D., Semmnov S.L., Stepanov S.G., Trofimov V.A., Yalovoi V.I. *Quantum Electron*., **45**, 415 (2015) [*Kvantovaya Elektron*., **45**, 415 (2015)].
11. Grudtsyn Ya.V., Koribut A.V., Trofimov V.A., Mikheev L.D. *J. Opt. Soc. Am. B*, **35**, 1054 (2018).
12. Grudtsyn Ya.V., Koribut A.V., Mikheev L.D., Trofimov V.A. *Quantum Electron*., **48**, 306 (2018) [*Kvantovaya Elektron*., **48**, 306 (2018)].
13. Bespalov V.I., Talanov V.I. *Pis'ma Zh. Eksp. Teor. Fiz*., **3**, 471 (1966).
14. Brabec T., Krausz F. *Phys. Rev. Lett*., **78**, 3282 (1997).
15. Skupin S., Bergé L. *Phys. D: Nonlinear Phenomena*, **220**, 14 (2006).
16. Malitson I.H. *J. Opt. Soc. Am*., **55**, 1205 (1965).
17. Levenson M. *IEEE J. Quantum Electron*., **10**, 110 (1974).
18. Malitson I.H. *Appl. Opt*., **2**, 1103 (1963).
19. DeSalvo R., Said A.A., Hagan D.J., Van Stryland E.W., Sheik-Bahae M. *IEEE J. Quantum Electron*., **32**, 1324 (1996).